

Low pressure chemical vapor deposition synthesis of hexagonal boron nitride on polycrystalline metal foils

Ashley Gibb^{1,2,3}, Nasim Alem^{2,3}, and Alex Zettl^{*2,4}

¹ Department of Chemistry, University of California, Berkeley, CA 94720, USA

² Department of Physics, University of California, Berkeley, CA 94720, USA

³ Materials Sciences Division, Lawrence Berkeley National Laboratory, Berkeley, CA 94720, USA

⁴ National Center for Electron Microscopy, Lawrence Berkeley National Laboratory, Berkeley, CA 94720, USA

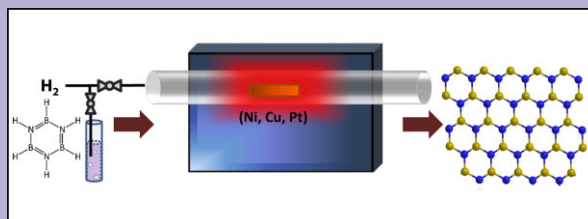
Received 16 April 2013, revised 14 August 2013, accepted 3 September 2013

Published online 11 October 2013

Keywords chemical vapor deposition, h-BN, hexagonal boron nitride

* Corresponding author: e-mail azettl@berkeley.edu, Phone: +01 510 642 4939, Fax: +01 510 643 8497

The two-dimensional sp^2 -bonded material hexagonal boron nitride (h-BN) has unique electronic, thermal, mechanical, and chemical properties. It has recently found use as an ideal substrate for graphene-based electronic devices. We here describe synthesis of mono- to few-layer h-BN films using low pressure chemical vapor deposition (LPCVD) from borazine, with nickel, copper and platinum employed as catalytic substrates, and transfer of some of these films using a non-polymer method. Characterization of the films via Raman spectroscopy and transmission electron microscopy (TEM) is performed.



Chemical vapor deposition synthesis of hexagonal boron nitride from borazine using metallic substrates.

© 2013 WILEY-VCH Verlag GmbH & Co. KGaA, Weinheim

1 Introduction Recent advances in the isolation of two-dimensional films have inspired much research on the development of stable self-supporting mono- and few-layer systems [1]. Most notably graphene, a single layer of hexagonal sp^2 carbon, has attracted interest due to intriguing electronic, optical, and mechanical properties [2]. Hexagonal boron nitride (h-BN) is a closely related two-dimensional material, isoelectronic with graphene but often exhibiting very different properties. Sheets of h-BN are atomically flat, inert, mechanically strong, and stable at high temperatures [3]. As a thermally but not electrically conducting material h-BN makes excellent substrates and dielectrics and has been investigated for use in future nanoscale devices [4]. Many different sp^2 -bonded BN-based materials have previously been synthesized, including layered crystals [5], sheets [6], nanoribbons [7, 8], cocoons [9], and nanotubes [10].

Although many fundamental studies of graphene, and to a much lesser extent, h-BN, have been performed using

mechanically exfoliated materials, such isolation methods are not practical on a large scale. Bulk liquid exfoliation from chemically modified graphene and h-BN pave the way for some applications [11], but the harsh oxidation processes are not completely reversible [12], resulting in high densities of sp^3 defects.

Much prior work has utilized ultra-high vacuum growths of h-BN on single crystals of transition metals [13, 14]. Although these methods have revealed much information about h-BN growth, structure, and properties [15–20], the use of extremely expensive single-crystal substrates hinders the scale of the synthesis. Additionally, single crystal substrates are not ideal for common transfer methods, which often require sacrificial etching of the metal.

Low pressure chemical vapor deposition (LPCVD) on polycrystalline substrates allows for facile growth of mono-layer graphene [21], and has been demonstrated to be highly scalable for device fabrication [22]. However, h-BN has proven

to be more synthetically challenging than graphene [23, 24]. In this paper, we discuss the synthesis of h-BN on various polycrystalline metallic substrates using LPCVD.

2 Experimental

2.1 Synthesis Mono- to few- layer h-BN was synthesized using LPCVD. Catalytic substrates of polycrystalline nickel (25 μm , 99.99%, Alfa Aesar), copper (25 μm , 99.8%), and platinum foil (0.1 mm, 98%) were utilized. Although we have successfully synthesized h-BN via the thermal decomposition of solid ammonia borane into either aminoborane or borazine (Fig. 1a), this process leads to a much more varied flow rate [25]. Using pure borazine provides greater control of the precursor dosage and film thickness. In these experiments, borazine was bubbled at a temperature of -15°C and a pressure of <3 mTorr. The flow rate is easily controlled by both a needle valve and a cold trap at the precursor. Figure 1b shows a schematic of the CVD process. Before growth, foils were exposed to UV and ozone at 100°C for 12 min, then annealed at 1020°C for 1 h under 100 sccm of hydrogen to remove surface oxides and contaminants. Growth occurred at 950°C over 15 min.

2.2 Transfer In order to further characterize sheets of h-BN, it is necessary to transfer them from their catalytic growth substrates using either a direct transfer [26] or a poly(methyl methacrylate) (PMMA) support.

Transmission electron microscopy (TEM) sample preparation was accomplished using a direct transfer without PMMA, detailed in Fig. 2. A drop of isopropyl alcohol was placed on the metal foil after h-BN growth. A TEM grid (Quantifoil R 1.2/1.3, gold support) was then placed on top of the liquid, allowing surface tension to adhere the grid to

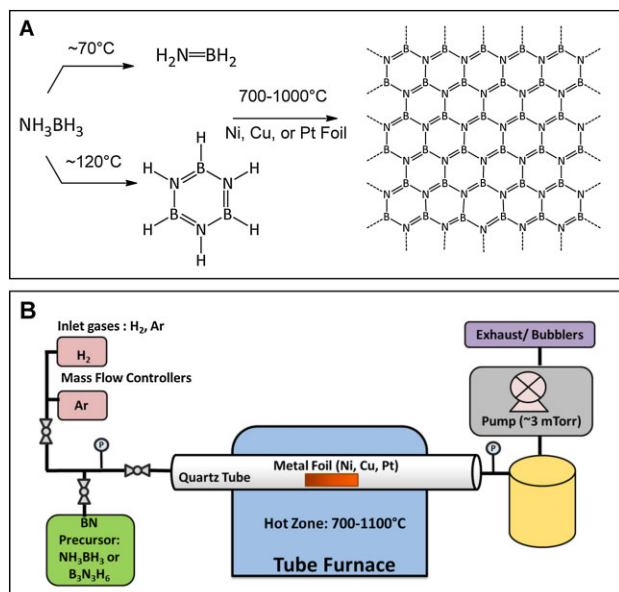


Figure 1 Synthesis of h-BN from ammonia borane or borazine (a). Chemical vapor deposition schematic (b).

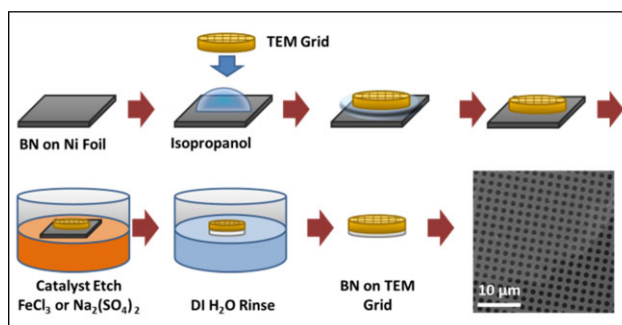


Figure 2 Direct transfer of h-BN on metal foil to a TEM grid (a). SEM image of transferred BN film on quantifoil grid (b).

the sample. The foil was subsequently floated for 3–5 h in a bath of iron chloride (0.1 g mL^{-1}) to etch the nickel samples, or sodium persulfate (0.15 g mL^{-1}) to etch the copper samples. The grid support structure was protected from the etchant by the h-BN.

To transfer h-BN to Si/SiO₂ substrates, a support film of PMMA was spin-coated onto the sample after growth. Nickel and copper metals were etched as above. For platinum, electrochemical exfoliation similar to that employed for graphene, and more recently h-BN, allowed for separation of the h-BN/PMMA film from the underlying platinum substrate [27–29]. The PMMA can then be dissolved in several baths of hot acetone. We found that even after several acetone baths, isopropanol rinses, and mild annealing some residues of polymer still remained. Alternative polymers such as polydimethylsiloxane may also prove to be useful transfer materials [30, 31], but the higher rigidity may inhibit electrochemical transfer. After removing the h-BN, the platinum foil was heated in air at 1100°C for 4 h then reused for multiple syntheses.

3 Characterization Raman data were collected on a Reinschaw inVia at 633 nm. TEM was performed on a JEOL 2010 operating at 80 kV. Atomic resolution images were obtained on the TEAM 0.5 microscope at the National Center for Electron Microscopy operating at 80 kV with a monochromated beam and spherical aberration correction to 5th order, yielding a spatial resolution below 1 Å.

3.1 Raman The E_{2g} phonon mode in h-BN leads to a characteristic Raman shift of 1367 cm^{-1} [32]. This shift originates from the fundamental stretching mode in the boron-nitrogen bond. Figure 3A shows the Raman spectra of h-BN grown on Ni, Cu, and Pt, with the characteristic h-BN peak at 1370 cm^{-1} . Raman signals were present across the entire sample, generally several centimeters in length, confirming large area coverage. We did not observe any difference between h-BN grown on pristine and reused platinum foils. Signal intensity was highest on the nickel sample. A higher signal intensity could arise from multiple factors such as a thicker film, higher crystallinity, or optical effects with the substrate. Therefore, the full width half

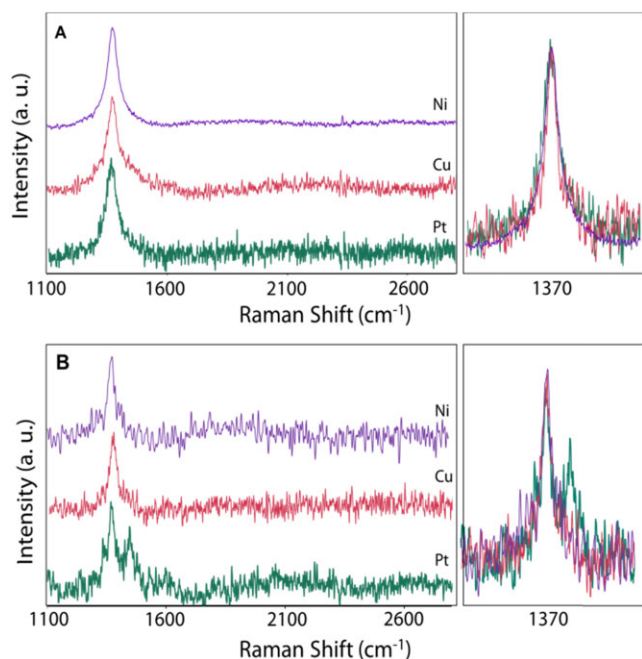


Figure 3 Raman spectra of h-BN synthesized on nickel (purple), copper (red), and platinum (green) foils on the metal substrate (a), and after transfer to SiO₂ (b). Insets show superimposed E_{2g} peaks at 1370 cm⁻¹.

maximum is helpful to characterize the quality of the films. Our experiments show a similar full width half maximum of 50.8, 45.5, and 47.1 cm⁻¹ for h-BN grown on Pt, Cu, and Ni, respectively, which suggests comparable sample quality. The Ni peak is the most symmetric, while the Cu peak exhibits some asymmetry. We note that h-BN can have different interactions with Ni, Cu, and Pt. In particular, the d orbital of the transition metal can perturb the BN monolayer. For Ni(111) substrates this results in a small charge displacement of 0.06 electrons from BN to Ni, in turn changing the work function of the metal [20]. Additionally, due to lattice mismatch, h-BN grown on some single crystal substrates will display a moiré pattern, revealed for example in STM measurements where a “nanomesh” results [20]. To eliminate such extraneous effects and to determine whether the Raman FWHM or asymmetry described above is related to metal substrate interactions, Raman measurements were additionally carried out on samples transferred to SiO₂, as shown in Fig. 3B. After transfer, the FWHM was measured to be 40.9, 36.9, and 29.8 cm⁻¹ on Pt, Cu, and Ni, respectively. The second peak in the Pt-derived sample at ~1450 cm⁻¹ has been observed previously [28, 29] in similarly transferred samples, and is likely due to PMMA residue. This supports further the advantage of using a non-PMMA transfer method.

3.2 Transmission electron microscopy TEM was used to probe the structure and crystallinity of our samples grown on Ni and Cu. Figure 4 shows TEM images of the film

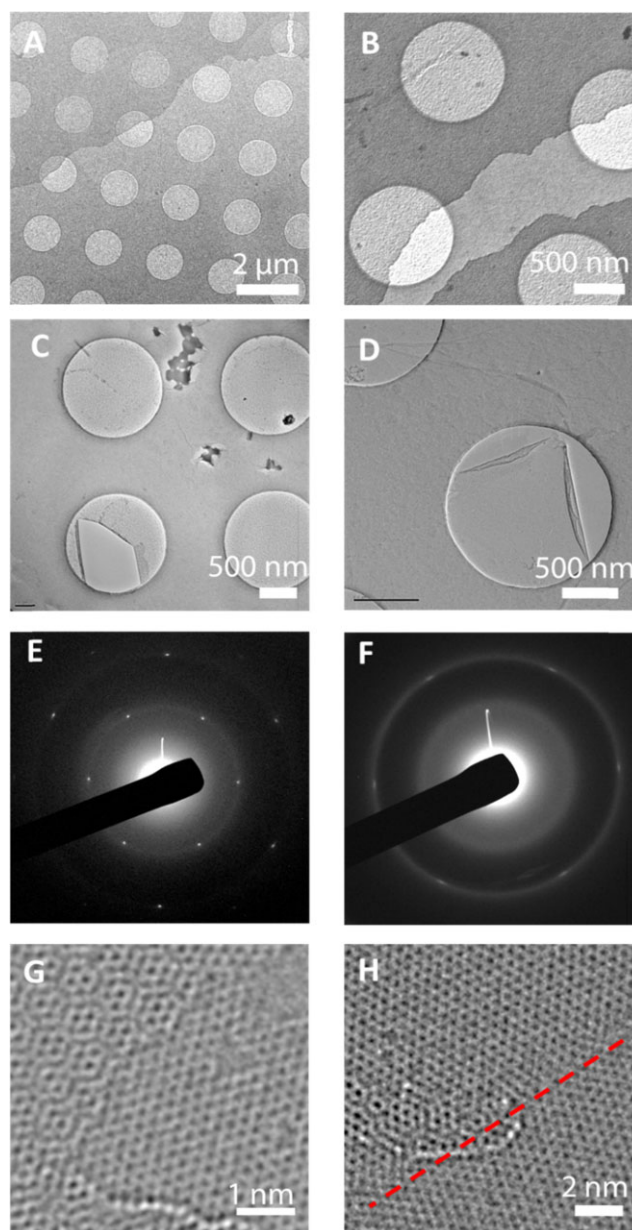


Figure 4 TEM bright field images of h-BN synthesized on Cu (a, b) and of h-BN synthesized on Ni (c, d). Diffraction pattern of h-BN synthesized from Ni (e), and Cu (f). Atomic resolution TEM images of h-BN synthesized on Ni foil: (g) few-layer region with vacancy defects; (h) grain boundary defects in monolayer h-BN.

synthesized on a copper substrate (a–b), and on a nickel substrate (c–d). Wrinkles, folds, and tears are readily observed on a thin, few-layer sheet. The diffraction pattern from nickel growth in Fig. 4e shows clear, sharp spots indicating a highly crystalline hexagonal film. In contrast, although the diffraction pattern of the film grown on copper does have hexagonal symmetry (Fig. 4f), the diffraction ring indicates a more amorphous structure. Indeed, under the same growth conditions the h-BN grown on nickel is thinner and cleaner, as can be seen via HRTEM in Fig. 4g–h.

Boron nitride exists in quite a number of solid phases other than h-BN, including cubic (c-BN), wurtzite (w-BN), turbostratic (t-BN), and rhombohedral (r-BN). Of these, c-BN and w-BN are sp^3 bonded, and the others are sp^2 bonded. According to calculations, c-BN is the most stable form of bulk boron nitride under ambient conditions, though the other forms are all metastable with high enough energy barriers to prevent transformation at room temperature [33]. However, we do not expect any c-BN to be present, nor have we seen any experimental data indicating the presence of c-BN in our samples. Theoretical calculations have shown that smaller clusters of h-BN are more stable than small clusters of c-BN, w-BN, or r-BN. Therefore, during a low to ambient pressure synthesis such as LPCVD, smaller clusters will nucleate to form sp^2 bonds rather than sp^3 bonds [34]. Thus it is quite unlikely that any c-BN or w-BN will be formed in a low or ambient pressure regime.

The formation of r-BN and t-BN however is much more probable, as these phases are closer in energy to h-BN. While h-BN is AA'AA' stacking with a *c*-axis of 6.6 Å, r-BN is ABCABC stacking with a *c*-axis of 10.01 Å (for 3 layers), and t-BN has random stacking with an interlayer distance approximately 3–4% larger than h-BN [34]. After monolayer growth is complete, interlayer forces will dominate the structural configuration. This typically yields h-BN with perfectly stacked commensurate layers. However, as these layers are not covalently bound, only held by van der Waals forces, it is possible for them to slide, thus forming either r-BN or t-BN. In our experiments we see predominately h-BN, but occasionally do observe some stacking mismatch (as in Fig. 4g). In Fig. 4g the bi-layer region exhibits a stacking offset, visible as a moiré pattern. However, the commensurate stacking in h-BN is lower in energy and dominates our samples.

Atomic resolution TEM also allowed for analysis of angstrom-scale defects in h-BN. Figure 4g shows a region of h-BN with vacancy defects, which are induced by electron beam irradiation during imaging [35]. These defects are primarily due to the ejection of a boron atom, due to its lower knock on threshold [36]. Figure 4h shows a region of monolayer h-BN with a grain boundary, highlighted in red. The misorientation angle of this grain boundary is approximately 22°. The atomic structure and dynamics of these grain boundary defects have been described in previous work [37]. These atomic scale defects are expected to be similar for h-BN grown on different substrates. Understanding these atomic-scale defects in h-BN is essential because they can affect macro-scale properties, key for developing device scale synthesis methods.

4 Conclusions The synthesis of h-BN via LPCVD on polycrystalline metal substrates deserves continued investigation, and may prove to be a reliable route towards generating large area films of h-BN. Non-PMMA transfer methods also show promise for relative clean manipulation of h-BN sheets. The low-pressure growth on Pt foils is

noteworthy in that the substrate is not consumed in the liftoff process.

Acknowledgements This work was supported in part by the Director, Office of Energy Research, Office of Basic Energy Sciences, Materials Sciences and Engineering Division, of the U.S. Department of Energy under Contract #DE-AC02-05CH11231 which provided for detailed TEM characterization, including that performed at the National Center for Electron Microscopy; the Office of Naval Research under MURI award N00014-09-1-1066 which provided for h-BN transfer; and the Air Force Office of Scientific Research under grant #FA9950-10-1-0451 which provided for CVD synthesis. AG acknowledges support from an NSF graduate research fellowship.

References

- [1] A. K. Geim and K. S. Novoselov, *Nature Mater.* **6**, 183 (2007).
- [2] C. N. R. Rao, A. K. Sood, K. S. Subrahmanyam, and A. Govindaraj, *Angew. Chem., Int. Ed. Engl.* **48**, 7752 (2009).
- [3] D. Golberg, Y. Bando, Y. Huang, T. Terao, M. Mitome, and C. Tang, *ACS Nano* **4**, 2979 (2010).
- [4] W. Gannett, W. Regan, K. Watanabe, T. Taniguchi, M. F. Crommie, and A. Zettl, *Appl. Phys. Lett.* **98**, 242105 (2011).
- [5] W. H. Balmain, *J. Prakt. Chem.* **27**, 422 (1842).
- [6] D. Pacilé, J. C. Meyer, C. O. Girit, and A. Zettl, *Appl. Phys. Lett.* **92**, 133107 (2008).
- [7] H. Zeng, C. Zhi, Z. Zhang, X. Wei, X. Wang, W. Guo, Y. Bando, and D. Golberg, *Nano Lett.* **10**, 5049 (2010).
- [8] K. J. Erickson, A. L. Gibb, A. Sinitiskii, M. Rousseas, N. Alem, J. M. Tour, and A. K. Zettl, *Nano Lett.* **11**, 3221 (2011).
- [9] J. Cumings and A. Zettl, *Chem. Phys. Lett.* **316**, 211 (2000).
- [10] N. G. Chopra, R. J. Luyken, K. Cherrey, V. H. Crespi, M. L. Cohen, S. G. Louie, and A. Zettl, *Science* **269**, 966 (1995).
- [11] S. Stankovich, D. Dikin, R. Piner, K. Kohlhaas, A. Kleinhammes, Y. Jia, and R. Ruoff, *Carbon* **45**, 1558 (2007).
- [12] C. Gómez-Navarro, R. T. Weitz, A. M. Bittner, M. Scolari, A. Mews, M. Burghard, and K. Kern, *Nano Lett.* **7**, 3499 (2007).
- [13] C. Oshima and A. Nagashima, *J. Phys.: Condens. Matter* **9**, 1 (1997).
- [14] A. B. Preobrajenski, A. S. Vinogradov, and N. Martensson, *Surf. Sci.* **582**, 21 (2005).
- [15] I. Shimoyama, Y. Baba, T. Sekiguchi, and K. G. Nath, *Phys. Status Solidi C* **9**, 1450 (2012).
- [16] A. B. Preobrajenski, A. S. Vinogradov, M. L. Ng, E. Cavar, R. Westerstrom, A. Mikkelsen, E. Lundgren, and N. Martensson, *Phys. Rev. B* **75**, 245412 (2007).
- [17] I. Shimoyama, Y. Baba, T. Sekigushi, and K. G. Nath, *J. Electron Spectrosc. Relat. Phenom.* **573**, 137 (2004).
- [18] A. Nagashima, N. Tejima, Y. Gamou, T. Kawai, and C. Oshima, *Phys. Rev. B* **51**, 4606 (1995).
- [19] A. Nagashima, N. Tejima, Y. Gamou, T. Kawai, and C. Oshima, *Phys. Rev. Lett.* **75**, 3918 (1995).
- [20] W. Auwärter, T. J. Kreutz, T. Greber, and J. Osterwalder, *Surf. Sci.* **429**, 229 (1999).
- [21] X. Li, W. Cai, J. An, S. Kim, J. Nah, D. Yang, R. Piner, A. Velamakanni, I. Jung, E. Tutuc, S. K. Banerjee, L. Colombo, and R. S. Ruoff, *Science* **324**, 1312 (2009).
- [22] S. Bae, H. Kim, Y. Lee, X. Xu, J. S. Park, Y. Zheng, J. Balakrishnan, T. Lei, H. R. Kim, Y. I. Song, Y. J. Kim, K. S.

- Kim, B. Ozyilmaz, J. H. Ahn, B. H. Hong, and S. Iijima, *Nature Nanotechnol.* **5**, 574 (2010).
- [23] Y. Shi, C. Hamsen, X. Jia, K. K. Kim, A. Reina, M. Hofmann, A. L. Hsu, K. Zhang, H. Li, Z. Y. Juang, M. S. Dresselhaus, L. J. Li, and J. Kong, *Nano Lett.* **10**, 4134 (2010).
- [24] K. K. Kim, A. Hsu, X. Jia, S. Kim, Y. Shi, M. Dresselhaus, T. Palacios, and J. Kong, *ACS Nano* **6**, 8583 (2012).
- [25] L. Song, L. Ci, H. Lu, P. Sorokin, C. Jin, J. Ni, A. Kvashnin, D. Kvashnin, J. Lou, B. Yakobson, and P. Ajayan, *Nano Lett.* **10**, 3209 (2010).
- [26] W. Regan, N. Alem, B. Alemán, B. Geng, C. Girit, L. Maserati, F. Wang, M. Crommie, and A. Zettl, *Appl. Phys. Lett.* **96**, 113102 (2010).
- [27] L. Gao, W. Ren, H. Xu, L. Jin, Z. Wang, T. Ma, L.-P. Ma, Z. Zhang, Q. Fu, L.-M. Peng, X. Bao, and H.-M. Cheng, *Nature Commun.* **3**, 699 (2012).
- [28] Y. Gao, W. Ren, Z. Ma, Z. Liu, Y. Zhang, W. B. Liu, L. P. Ma, X. Ma, and H. M. Cheng, *ACS Nano* (2013), DOI: 10.1021/nn4009356.
- [29] G. Kim, A. R. Jang, H. Y. Jeong, Z. Lee, D. J. Kang, and H. S. Shin, *Nano Lett.* **13**, 1834 (2013).
- [30] S. J. Kang, B. Kim, K. S. Kim, Y. Zhao, Z. Chen, G. H. Lee, J. Hone, P. Kim, and C. Nuckolls, *Adv. Mater.* **23**, 3531 (2011).
- [31] K. S. Kim, Y. Zhao, H. Jang, S. Y. Lee, J. M. Kim, K. S. Kim, J. H. Ahn, P. Kim, J. Y. Choi, and B. H. Hong, *Nature* **457**, 706 (2009).
- [32] T. Kuzuba, K. Era, T. Ishii, and T. Sato, *Solid State Commun.* **25**, 863 (1978).
- [33] P. K. Lam, International Conference on High Pressure Science and Technology (AIRAPT-17), Poster Session IV, Honolulu, HI, USA, 1999.
- [34] M. G. Balint and M. I. Petrescu, *Diam. Relat. Mater.* **18**, 1157 (2009).
- [35] N. Alem, R. Erni, C. Kisielowski, M. Rossell, P. Hartel, B. Jiang, W. Gannett, and A. Zettl, *Phys. Status Solidi RRL* **5**, 295 (2011).
- [36] J. Kotakoski, C. Jin, O. Lehtinen, K. Suenaga, and A. Krasheninnikov, *Phys. Rev. B* **82**, 1 (2010).
- [37] A. L. Gibb, N. Alem, J. H. Chen, K. J. Erickson, J. Ciston, A. Gautam, M. Linck, and A. Zettl, *J. Am. Chem. Soc.* (2013), DOI: 10.1021/ja400637n.